ChemComm

COMMUNICATION

View Article Online
View Journal | View Issue

Cite this: *Chem. Commun.*, 2022, **58**, 5249

Received 7th February 2022,
Accepted 31st March 2022

DOI: 10.1039/d2cc00772j

rsc.li/chemcomm

Effect of Na^+ and K^+ on the cucurbituril-mediated hydrolysis of a phenyl acetate†

Nazar Rad * and Volodymyr Sashuk *

The environment around the active site affects the catalytic activity of enzymes. Studying the cucurbit[7]uril-promoted acid hydrolysis of a cationic phenyl acetate derivative, we found that the hydrophobic cavity of the macrocycle screens the reaction centre from the positively charged neighbouring group. Moreover, the chelation of alkali metal cations with the cucurbit[7]uril portal and acetyl group of the substrate reduces the hydrolysis rate of the encapsulated ester in an aqueous solution. This type of inhibition corresponds to a rare uncompetitive model in contrast to the more common competitive model that relies on substrate displacement.

Sodium and potassium are the most abundant cations in living cells. Due to the ion-specific proteins embedded into the membrane, the concentration of potassium is much higher in the cell than in seawater (140 mM *vs.* 5 mM), while the sodium concentration is lower (30 mM *vs.* 140 mM). The cell utilizes this imbalance to regulate cell transport, volume maintenance and signal transduction. Sodium and potassium also play a specific role in the activation of some enzymes. These cations attract the substrate or directly affect the catalytic process as a cofactor, and optimize the conformation of the enzyme.[1,2] Alkali metal cations can also inhibit enzymatic processes.[3] When the enzyme is highly negatively charged (such as acetylcholinesterase), it is difficult to distinguish the ionic strength effect from the specific binding of the cation to the enzyme.[4] Therefore, the mechanism of cation action is not always clear.

Alkali metal cations can regulate the catalytic activity of a number of artificial enzymes.[5] These enzyme mimics contain a crown-ether moiety responsible for cation coordination. The attachment of the cation induces conformational changes that affect catalytic activity.[6–8] Notably, the developed artificial enzymes operate in non-aqueous media because of the low solubility of crown-ether in water. The ion-specific effect of the cation on the enzyme functionality in an aqueous medium is attenuated by solvation.[9,10] Here we demonstrate for the first time that the coordination of alkali metal cations (Li^+, Na^+, K^+ and Cs^+) can affect the activity of an artificial enzyme even in water.

In our study, we used a water-soluble cucurbit[7]uril macrocycle (**CB7**). Like natural enzymes, cucurbiturils create stable binary complexes with certain organic guests and accelerate their chemical transformation.[11] The portals of these macrocycles also attract metal cations.[12] The coordination of a cation can either prevent the substrate encapsulation[13] or lead to the formation of a ternary complex[14] altering the position of the encapsulated guest inside the macrocyclic cavity (Na^+ and Ag^+).[18,19] Transition metal cations coordinated to cucurbiturils promote desilylation (Ag^+),[15] and increase the chemoselectivity of deazotation (Ag^+)[16] and the enantioselectivity of Diels–Alder reaction (Cu^{2+}).[17]

The catalytic activity of neat cucurbiturils can be rationalized by the excess electronic density on the two portals that accumulate hydroxonium ions around the reaction centre.[18] These macrocycles promote the hydrolytic cleavage of amides,[19] benzoyl chlorides,[20] esters,[21] ethers,[18] triazenes,[22] oximes,[19] and Schiff bases,[23] as well as the formation of hydrazones.[24]

As a model reaction we choose the acid hydrolysis of esters (Scheme 1). This reaction is slow enough for observation at low pH. The rate of hydrolysis depends on the concentration of the tetrahedral intermediate **TI**, which increases with increasing concentration of ester conjugated acid **PhAc·H**.[25,26] We expected **CB7** to promote hydrolysis by enhancing the basicity of the encapsulated substrate.[27,28] Although ester hydrolysis is a reversible process, the excess of water molecules almost

Institute of Physical Chemistry, Polish Academy of Sciences, Kasprzaka 44/52, 01-224 Warsaw, Poland. E-mail: nrad@ichf.edu.pl

† Electronic supplementary information (ESI) available: Details of experimental procedures, spectral data, and analytical data. See **https://doi.org/10.1039/d2cc00772j**

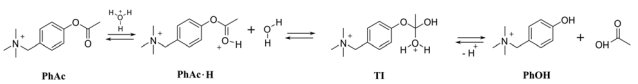

Scheme 1 Acid hydrolysis of **PhAc**.

completely shifts the equilibrium towards product formation. The employed acetate derivative (**PhAc**) is reminiscent of the neurotransmitter acetylcholine, the concentration of which at the synapse is controlled by the hydrolytic enzyme acetylcholinesterase. As in the case of acetylcholine, a positively charged ammonium group was expected to facilitate complexation.

Initial experiments were performed in an aqueous solution of acid in the absence of any metal cations to avoid the competition of cations with the substrate. The binding constant of **PhAc** with **CB7** determined by ^{1}H NMR titration is equal to $(1.5 \pm 0.42) \times 10^5$ M^{-1}. The addition of **CB7** to **PhAc** shifts all proton signals upfield (ESI† Fig. S2). The most shifted signal belongs to aromatic proton 3c in the meta-position to the acetate group. Significantly shifted are also the proton resonances of ammonium group 5c. The less shifted signal corresponds to the proton of acetate group 1c. Based on this, we can conclude that the phenyl ring and ammonium group are buried deep inside the cavity, and the acetate group is localised close to one of the **CB7** rims (Fig. 1a).

In the salt-free solution, the hydrolysis rate of **PhAc** k_f depends linearly on the concentration of H_3O^+ ions in the range of pH between 0.75 and 2.5 (Fig. 1b). Since both **PhAc** and H_3O^+ involved in the formation of the transition state are positively charged species, k_f depends also on the ionic strength of the solution (eqn (1)). A similar positive salt effect has already been noted in the hydrolysis of acetylcholine in acid solution.[29]

$$k_f = k_f^0 \cdot [D^+] \cdot 10^{-2\cdot\left(-\frac{0.509\cdot\sqrt{I}}{1+\sqrt{I}} + 0.14\cdot I\right)} \quad (1)$$

where k_f^0 stands for the hydrolysis rate constant of free **PhAc**, $[D^+]$ denotes the concentration of deuterium ions, and I is the ionic strength.

Adding 1.1 eq of **CB7** to **PhAc** accelerates the reaction by more than two orders of magnitude. In this case, the rate of hydrolysis k_b increases linearly (Fig. 1b) as pH decreases following eqn (2).

$$k_b = k_b^0 \cdot [D^+] \quad (2)$$

where k_b^0 is the rate constant of **CB7**-promoted hydrolysis.

The slope of $\log k_b$ *versus* $\log[D^+]$ is equal to unity (Fig. S6b, ESI†). Thus, the rate of **CB7**-mediated hydrolysis is insensitive to the ionic strength of the solution. The lack of the primary salt effect for encapsulated **PhAc** is explained by the presence of the hydrophobic cavity that screens the reaction centre (acetate group) from the charged anchor (ammonium group).

The efficiency of the macrocycle as a catalyst can be assessed by the acceleration factor α. The acceleration factor, calculated as the ratio of the hydrolysis rate constants of the encapsulated and free **PhAc** (eqn (3)), decreases as the ionic strength of the solution increases. That is, if the substrate is charged, the ionic-strength-independent acceleration factor α^0 should be given instead. For **CB7**-promoted **PhAc** acid hydrolysis, α^0 is equal to 263 ± 11.

$$\alpha = \frac{k_b}{k_f} \quad (3)$$

Assuming that the acceleration effect of **CB7** is due to an increase in substrate basicity, the concentration of **PhAc@CB7·H** should be 263 times higher than the concentration of **PhAc·H** at the same pH. Since almost all substrate (96%) is encapsulated by **CB7** and the concentration of protonated ester is very low (pK_a is equal about −7), the concentrations of free (**PhAc**) and encapsulated substrate (**PhAc@CB7**) should be practically the same under reaction conditions. Thus, the found α^0 should correspond to the ratio between the basicities of the free and encapsulated substrate (eqn (4)).

$$\frac{K_{a,f}}{K_{a,b}} = \frac{[H^+]\cdot[PhAc]}{[PhAc\cdot H]} \cdot \frac{[PhAc@CB7\cdot H]}{[H^+]\cdot[PhAc@CB7]} \approx \frac{[PhAc@CB7\cdot H]}{[PhAc\cdot H]} \approx \alpha^0 \quad (4)$$

$$\Delta pK_a = pK_{a,b} - pK_{a,f} = \log K_{a,f} - \log K_{a,b} = \log\frac{K_{a,f}}{K_{a,b}} \approx \log\alpha^0 \approx 2.42 \quad (5)$$

where $K_{a,f}$ and $K_{a,b}$ are the acidity constants of the conjugated acid of free and encapsulated ester.

The logarithm of α^0 is equal to 2.42 (eqn (5)) which is in the range of typical **CB7**-induced pK_a shifts (2–3).[27,28] This confirms our assumption that the stabilization of the ester conjugated acid by **CB7** is the main reason for accelerated hydrolysis.

In the next step, we studied the effect of alkali metal ions. The addition of sodium chloride sped up the hydrolysis of free **PhAc** due to the increase of ionic strength and reduced the activity of **CB7**. The obtained kinetic data do not agree with competitive inhibition, where the sodium cation competes with the substrate for the macrocycle (Fig. 2b).

Moreover, the competitive inhibition scenario does not explain the shifts in the ^{1}H NMR spectrum. Upon adding salt, the signal of the 2c proton moves upfield, which can only be accounted for by the translocation of the phenyl ring deeper into the **CB7** cavity (Fig. 3b).

To elucidate the source of inhibition, we recorded NMR spectra in the presence of alkali metal halides. The analysis has shown that the shielding of 2c proton signals depends strongly on the nature of the cation (ESI† Fig. S7) and does not change when varying the anion (ESI† Fig. S8). This observation is

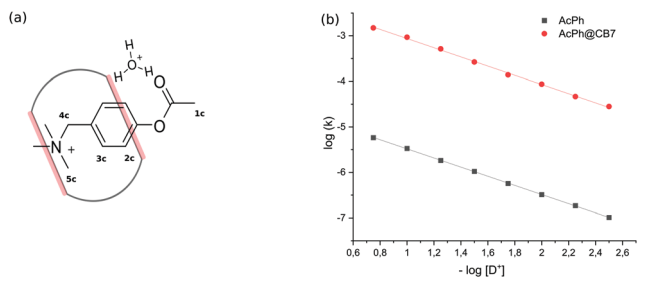

Fig. 1 (a) Schematic depiction of transition state stabilization by **CB7** portals. (b) pD-profiles of acid hydrolysis of **PhAc** (1.5 mM) and **PhAc@CB7** (1.5 mM).

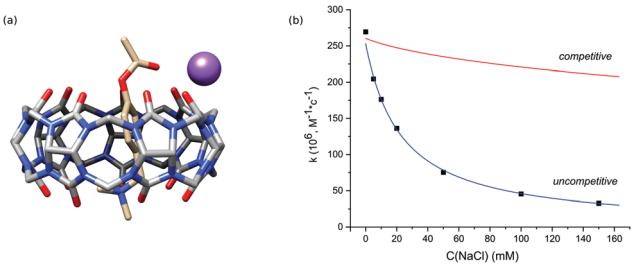

Fig. 2 (a) PM6-optimized structure of the **PhAc@CB7·Na** ternary complex. The sodium ion coordinates with oxygen atoms of two ureido groups of **CB7** and the acetyl group of **PhAc**. (b) The sodium cation effect on the hydrolysis rate constant of **PhAc@CB7**. Experimental data fit the model of uncompetitive inhibition.

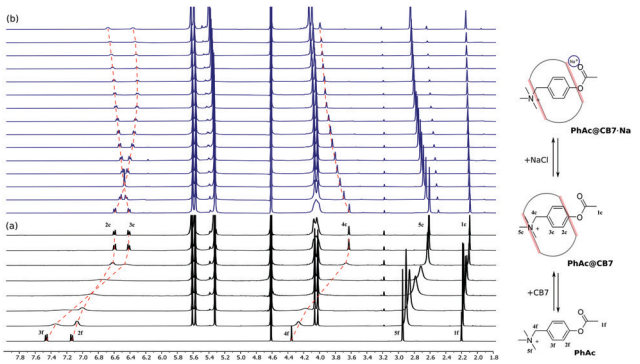

Fig. 3 (a) NMR titration experiments of free **PhAc** (1.5 mM) with **CB7** (0–1.65 mM) and (b) the **PhAc@CB7** complex (2.0–1.4 mM) with NaCl (0–460 mM). The concentration of CB7 and NaCl increases from the bottom up. The signals of two aromatic hydrogen atoms 2c and 3c coalesce at the concentration of NaCl equal to 10 mM.

supported by acceleration factors α_{CB7}, which differ markedly for four cations, and are of practically the same value for four anions (Table 1).

Thus, we consider the model of uncompetitive inhibition of **CB7** by the cation. According to this model, the cation binds to the **CB7** portal next to the reactive centre to afford a **PhAc@CB7·Na** ternary complex (Fig. 2a). The positively charged alkali cation decreases the concentration of conjugated acid of ester **PhAc@CB7·H** to slow down the acid hydrolysis. The formation of the ternary complex is supported by the mass analysis of the isolated **PhAc@CB7** complex revealing a monosodium doubly charged molecular ion (ESI† Fig. S21).

The kinetic data of **PhAc@CB7** hydrolysis in the presence of different amounts of sodium chloride (Fig. 2b) were employed to estimate the **PhAc@CB7** affinity for the sodium cation according to the model of uncompetitive inhibition. The obtained binding constant is almost identical to the constant determined by NMR titration within the statistical error (Table 2). Thus, the deactivation of **CB7** correlates with the cation-induced dislocation of the macrocycle toward the ester group.

The binding constants calculated for other cations also yield very close values for both methods. The cation affinity for the **PhAc@CB7** complex (Table 2) decreases in the same order as the inhibition efficiency of the cations: $Na^+ > K^+ > Cs^+ > Li^+$ (Fig. 4, ESI† Table S3).

The **PhAc@CB7** complex binds sodium two times stronger than pure **CB7** ($K = 21 \pm 2$ M^{-1}).[30] This indicates that the organic guest reinforces the binding. The replacement of substrate **PhAc** by the product **PhOH** changes the affinity of the **CB7**-guest complex for cations. As with the substrate, the NMR shifts of the product **PhOH@CB7** depend on the concentration of cations (ESI† Fig S11, S14, S16 and S18). The determined binding constants of **PhOH@CB7** with cations decrease in the order $K^+ > Cs^+ > Na^+ > Li^+$ (Fig. 4). The similarity between the sodium affinity to free **CB7** and **PhOH@CB7** shows that, in contrast to the acetyl group, the hydroxyl group is not involved in the coordination of sodium cations. Thus, both cucurbit[7]uril and the substrate are involved in cation coordination.

To summarise, we scrutinised the effect of ionic strength on ester hydrolysis mediated by cucurbit[7]uril. In the absence of inorganic salts, the macrocycle screens the reaction centre from the cationic anchor making the substrate and the macrocycle insensitive to the ionic strength of the solution. However, after the addition of salts, the catalytic activity of the macrocycle is suppressed. The reason for this is the formation of a ternary complex with alkali metal cations that is less susceptible to hydronium ion attack. This type of inhibition can be described by the uncompetitive model in which the substrate remains bound

Table 1 Hydrolysis rate constants of **PhAc@CB7** (1.5 mM) in the presence of different salts (10 mM) at pD of 1.55

Salts	$k_{f,M} \times 10^6$, M^{-1} s^{-1}	$k_{b,M} \times 10^6$, M^{-1} s^{-1}	$k_{f,M}/k_{f,0}$	$k_{b,M}/k_{b,0}$	α_{CB7}
salt-free	1.3	269.4	1.0	1.0	207
Cation effect					
LiCl	1.28	268.0	1.0	1.0	210
NaCl	1.25	180.9	1.0	0.7	145
KCl	1.27	183.7	1.0	0.7	145
CsCl	1.24	229.9	1.0	0.9	185
Anion effect					
NaF[a]	0.83	117.1	0.6	0.4	141
NaCl	1.25	180.9	1.0	0.7	145
NaBr	1.33	179.6	1.0	0.7	142
NaI	1.35	197.8	1.0	0.7	147

$k_{f,0}$ and $k_{b,0}$ correspond to the **PhAc** and **PhAc@CB7** hydrolysis rate constants under salt-free conditions. [a] Due to the buffering effect of NaF, the pD of the reaction mixture was higher.

Table 2 The binding constants K_a (M^{-1}) of alkali cations with **PhAc@CB7** and **PhOH@CB7**

Cation	**PhAc@CB7** kinetics data	**PhAc@CB7** NMR shifts	**PhOH@CB7** NMR shifts
Li^+	1.8 (0.7%)	1.1 (6.8%)	0.9 (4.5%)
Na^+	46 (2.0%)	46 (4.8%)	19 (3.6%)
K^+	42 (2.1%)	43 (6.7%)	30 (8.8%)
Cs^+	12 (2.3%)	11 (4.8%)	22 (11.5%)

Three binding constants for the cation were determined in one experiment. The numbers in parentheses show the relative mean deviation of the calculated data from the experimental ones.

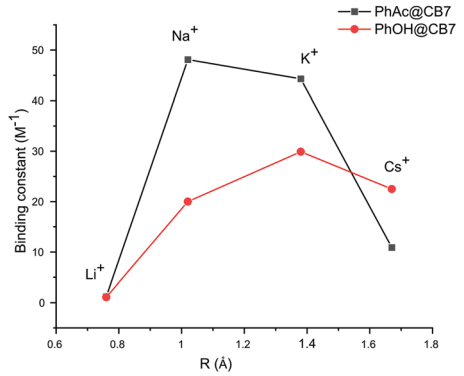

Fig. 4 Plots of binding constants *vs.* cation radius for substrate **PhAc@CB7** and product **PhOH@CB7** complexes.

to the macrocycle instead of being displaced by the inhibitor. This work shows that Na and K cations abundant in aqueous solutions can specifically modulate the operation of artificial enzymes. Moreover, the cation selectivity observed during the formation of ternary complexes can be the basis for the development of new cation receptors.

NR would like to thank the National Science Centre of Poland (grant MINIATURA 3 no 2019/03/X/ST4/01017) for funding the research and PLGrid Infrastructure for supporting the QM calculations.

Conflicts of interest

There are no conflicts to declare.

Notes and references

1 M. J. Page and E. Di Cera, *Physiol. Rev.*, 2006, **86**, 1049–1092.
2 M. Vasak and J. Schnabl, *Met. Ions Life Sci.*, 2016, **16**, 259–290.
3 H. Zhao, *J. Mol. Catal. B: Enzym.*, 2005, **37**, 16–25.
4 V. Tougu and T. Kesvatera, *Biochim. Biophys. Acta, Protein Struct. Mol. Enzymol.*, 1996, **1298**, 12–30.
5 C. Yoo, H. M. Dodge and A. J. M. Miller, *Chem. Commun.*, 2019, **55**, 5047–5059.
6 T. Tozawa, S. Tokita and Y. Kubo, *Tetrahedron Lett.*, 2002, **43**, 3455–3457.
7 G. H. Ouyang, Y. M. He, Y. Li, J. F. Xiang and Q. H. Fan, *Angew. Chem., Int. Ed.*, 2015, **54**, 4334–4337.
8 Y. J. Lee, K. S. Liu, C. C. Lai, Y. H. Liu, S. M. Peng, R. P. Cheng and S. H. Chiu, *Chem. – Eur. J.*, 2017, **23**, 9756–9760.
9 L. Escobar and P. Ballester, *Chem. Rev.*, 2021, **121**, 2445–2514.
10 P. S. Cremer, A. H. Flood, B. C. Gibb and D. L. Mobley, *Nat. Chem.*, 2018, **10**, 8–16.
11 B. H. Tang, J. T. Zhao, J. F. Xu and X. Zhang, *Chem. – Eur. J.*, 2020, **26**, 15446–15460.
12 S. Zhang, L. Grimm, Z. Miskolczy, L. Biczok, F. Biedermann and W. M. Nau, *Chem. Commun.*, 2019, **55**, 14131–14134.
13 C. Marquez, R. R. Hudgins and W. M. Nau, *J. Am. Chem. Soc.*, 2004, **126**, 5806–5816.
14 Z. Miskolczy, M. Megyesi, L. Biczok, A. Prabodh and F. Biedermann, *Chem. – Eur. J.*, 2020, **26**, 7433–7441.
15 X. Y. Lu and E. Masson, *Org. Lett.*, 2010, **12**, 2310–2313.
16 A. L. Koner, C. Marquez, M. H. Dickman and W. M. Nau, *Angew. Chem., Int. Ed.*, 2011, **50**, 545–548.
17 L. F. Zheng, S. Sonzini, M. Ambarwati, E. Rosta, O. A. Scherman and A. Herrmann, *Angew. Chem., Int. Ed.*, 2015, **54**, 13007–13011.
18 L. Scorsin, J. A. Roehrs, R. R. Campedelli, G. F. Caramori, A. O. Ortolan, R. L. T. Parreira, H. D. Fiedler, A. Acuna, L. Garcia-Rio and F. Nome, *ACS Catal.*, 2018, **8**, 12067–12079.
19 C. Klock, R. N. Dsouza and W. M. Nau, *Org. Lett.*, 2009, **11**, 2595–2598.
20 N. Basilio, L. Garcia-Rio, J. A. Moreira and M. Pessego, *J. Org. Chem.*, 2010, **75**, 848–855.
21 A. Fierro, L. Garcia-Rio, S. Arancibia-Opazo, J. J. Alcazar, J. G. Santos and M. E. Aliaga, *J. Org. Chem.*, 2021, **86**, 2023–2027.
22 V. Sashuk, H. Butkiewicz, M. Fialkowski and O. Danylyuk, *Chem. Commun.*, 2016, **52**, 4191–4194.
23 J. J. Alcazar, N. Geue, V. Valladares, A. Canete, E. G. Perez, L. Garcia-Rio, J. G. Santos and M. E. Aliaga, *ACS Omega*, 2021, **6**, 10333–10342.
24 N. Rad, O. Danylyuk and V. Sashuk, *Angew. Chem., Int. Ed.*, 2019, **58**, 11340–11343.
25 Z. Said and J. G. Tillett, *J. Org. Chem.*, 1981, **46**, 2586–2588.
26 C. A. Bunton, J. H. Crabtree and L. Robinson, *J. Am. Chem. Soc.*, 1968, **90**, 1258.
27 N. Basilio, S. Gago, A. J. Parola and F. Pina, *ACS Omega*, 2017, **2**, 70–75.
28 I. Ghosh and W. M. Nau, *Adv. Drug Delivery Rev.*, 2012, **64**, 764–783.
29 R. P. Bell and M. Robson, *Trans. Faraday Soc.*, 1964, **60**, 893.
30 H. Tang, D. Fuentealba, Y. H. Ko, N. Selvapalam, K. Kim and C. Bohne, *J. Am. Chem. Soc.*, 2011, **133**, 20623–20633.

